

RESEARCH ARTICLE

CoMP-JT Scheme for D2D Communication in Industrial LiFi Networks

AHMET BURAK OZYURT^{ID}, (Graduate Student Member, IEEE),
AND WASIU O. POPOOLA^{ID}, (Senior Member, IEEE)

School of Engineering, Institute for Digital Communications, The University of Edinburgh, Edinburgh EH9 3FD, U.K.

Corresponding author: Ahmet Burak Ozyurt (a.b.ozyurt@ed.ac.uk)

This work was supported by the European Union's Horizon 2020 Research and Innovation Program under the Marie Skłodowska Curie titled ENLIGHT'EM: European Training Network in Low-Energy Visible Light IoT Systems (<https://enlightem.eu/>) under Grant 814215.

ABSTRACT This paper focuses on the combined technique of device-to-device (D2D) and coordinated multipoint joint transmission (CoMP-JT) to bridge the indoor industrial wireless gap with LiFi-based networks. It also considers the mobility challenge of industrial Internet-of-Things (IIoT) within a realistic scenario. Using the semiangle at half illuminance of the LiFi access point and D2D transmitting IIoT, we derive a coverage model for the communication range. Using stochastic geometry, the analytical expressions for CoMP-JT probability and coverage performance are derived in terms of different parameters, such as transmitter densities and bias factor. The analytical approximations match quite well with the Monte Carlo method-based simulation results.

INDEX TERMS Coordinated multipoint joint transmission, device-to-device communication, Industrial Internet of Things, LiFi, visible light communication.

I. INTRODUCTION

The trend towards the fourth industrial revolution continues to gather momentum as billions of new industrial Internet-of-Things (IIoT) devices are connected to the global Internet. Radical shifts are taking place using modern smart technology such as large-scale machine-to-machine communication (M2M) and the IIoT. Especially, new use cases for IIoT networks have been introduced such as sensing and recording data, smart metering, logistic management, and monitoring for industrial applications [1]. According to a projection in [2], short-range IIoT connections could reach close to 21 million connections by 2025. Hence, the necessity of novel wireless technologies is inescapable because of upcoming use cases. At this point, LiFi - a light spectrum-based wireless system- emerges as a potential communication technology for enabling dense IIoT networks due to accurate indoor positioning, high throughput, high reliability, and low latency requirements of the IIoT [3].

The associate editor coordinating the review of this manuscript and approving it for publication was Rentao Gu^{ID}.

The device-to-device (D2D) communication and coordinated multipoint joint transmission (CoMP-JT) techniques offer opportunities to reap the aforementioned advantages of LiFi-based IIoT networks. D2D communication occurs when IoT devices transmit and receive data directly among themselves without the need for relaying through a base station (BS) or an access point (AP). Thus, D2D offers improvements in resource usage, energy efficiency and latency [4]. Existing D2D literature can be said to focus on two main approaches. The first approach combines radio frequency (RF) and visible light bands to maximize efficiency of the system. In this type of studies, authors proposed to use LiFi for D2D communication and RF for cellular communication, namely connection between IIoTs and APs. These type of hybrid networks are usually not preferred because they need a much longer processing time than conventional networks due to the change of air interfaces [5]. Moreover, the RF system provides lower system capacity than the LiFi network, and a very large number of RF users will significantly reduce efficiency. Due to these reasons, previous studies focus on improvements such as mode selection, resource allocation, and optimizations in hybrid D2D schemes [6]–[13].

Zhang *et al.* propose a hierarchical game framework for resource allocation in heterogeneous network with VLC and D2D individual [6], [10]. In the game, the data packet size, the price of licensed spectrum and data rates are determined with equilibrium solutions, and each VLC transmitter (VLCT) determines the optimal data transmission route. Najla *et al.* focus on a multi-objective optimization problem which is the selection between RF and VLC bands for D2D [11], [12]. In these studies, they propose low-complexity heuristic algorithm and deep neural network for solving the problem. The studies reported in [7], [8], [13] suggest dynamic dwell timer and graph theory-based algorithms, tailored for D2D communication, in deciding whether or not it is beneficial for a user equipment to switch from VLC to RF or vice versa. Finally, [9] proposes a reinforcement learning (RL)-based approach to determine data transmission routes in an indoor VLC-D2D heterogeneous network. The second approach relates to the use of the visible light band for both direct and D2D communications. In this approach, the direct communication is defined as the link between IoTs and APs, not IoTs to IoTs. A few studies reported on this model, which is more beneficial than hybrid networks because of the aforementioned reasons. Proposed and analyzed in [14] are ways to understand how increasing distance between IoT devices affects efficient D2D communication. In the same model, optical repeaters are suggested for enhancing the performance of D2D communications. In [15], the study proposes a game theory-based solution for the mode selection mechanism between direct and D2D communication. This work uses system capacity as the utility function to optimize system performance and selects the optimal communication mode. Chaleshtori *et al.* investigate D2D communications using smart phones' display pixels and their built-in cameras [16], [17]. The impact of the receiver orientation on the channel characteristics is also investigated, where two static users face each other and the receiver is intentionally oriented towards the transmitter. Finally, in [18], the challenges and applications of LiFi in D2D communication are given briefly and LiFi is compared with other D2D communication options such as WiFi and Zigbee.

CoMP-JT is an inter-cell cooperation technology in which data to a receiver is concurrently transmitted from multiple transmitters to increase the received signal strength [19]. CoMP-JT scheme uses multiple APs to jointly transmit the data at the same time-frequency resource and by that converts interfering signals into useful signals. In addition, CoMP-JT scheme can achieve high gains in system throughput, robustness to blockage, and coverage probability. The indoor deployment of LiFi networks can benefit from power-line communication (PLC) as a backhaul solution to support coordination and data exchange among cooperating APs in CoMP-JT operations. The previous CoMP-JT studies in LiFi networks have many similarities in terms of system models [20]–[25]. All of these studies assume that transmitters have fixed locations and are identical. These studies are differentiated in regard to applied algorithms and proportional

fairness scheduling schemes. Besides, most of them are simulation-based with no analytical framework to back up the simulations.

To the authors' best knowledge, the combination of D2D communication and CoMP-JT scheme for mobile IIoT devices in LiFi networks has not been studied in any previous work. This paper investigates the role of mobile IIoT devices for D2D communication and CoMP-JT scheme in industrial LiFi networks using stochastic geometry. This work is based on a realistic scenario as contained in 'Scenario 4: Manufacturing Cell in LiFi standards, produced by the IEEE 802.11bb Task Group on Light Communication [26]. The major contributions of this paper are summarized as follows:

- We present an analytical modelling of CoMP-JT scheme for D2D communication range for IIoT devices based on the system parameters such as access point densities and half-angle of transmitters.
- Closed-form approximations are derived for the probability of CoMP-JT scheme for LiFi-based D2D networks in terms of ROI.
- Extensive Monte-Carlo based simulations presented to validate the analytical model.
- The impact of system parameters, such as transmitter density on the communication performance is investigated and inferences drawn. This is vital towards the design of a practical industrial LiFi network.

The remainder of the work is organized as follows. In the next section, the network model and LiFi channel model is introduced as parts of the system model. In Section III and IV, the CoMP-JT probability for LiFi networks and coverage performance with analytical expressions are presented. Simulation to verify the analytical results are shared in Section V. Section VI, finally, presents the concluding remarks and future research directions.

II. SYSTEM MODEL

This section provides the network model for CoMP-JT enabled D2D communication for mobile IIoT devices which is used in the study. First, Poisson Point Process (PPP) model with the Poisson-Voronoi tessellation (PVT) is used to distribute the IIoT devices and APs. Then, the details of the LiFi channel model used in the study are given.

A. NETWORK MODEL

In most previous studies about LiFi networks, cell shapes are modeled as either hexagonal or square. However, the ultra-dense industrial LiFi networks generally consist of a number of 'statistically random' APs and IIoT devices, such as sensors, robotic arms, drones, surveying and inspection machines, and even automatic guided vehicles (AGV) [27], [28]. Thus, using a perfectly defined deterministic/regular model for the positioning of these IIoT devices and APs is impractical. Spatial point process is therefore considered to provide a more accurate and tractable model for the distribution of nodes in an industrial LiFi network.

That should be highlighted that a LiFi AP is used as both illumination and data source which is different to the conventional RF nodes. Thus, LiFi networks cannot follow exactly the same assumptions used in RF network design. In RF networks, the minimum distance between nodes provides a more realistic process, e.g. Matérn Hard-Core Process (MHCP). However, it has been reported that the deployment of LiFi APs is completely random due to the wiring complexity, uncertain lighting requirements, and aesthetic quality [29]. In addition, other point process models, such as hardcore point process and square networks, are lower bounded by the PPP model [30]. For these reasons, we consider the PPP model as a worst-case deployment scenario for the industrial LiFi networks.

A PPP is a type of random mathematical object that consists of points randomly located on a mathematical space with parameter λ (means density) [31]. The number of points in any compact cluster $B \subset R^d$ is a Poisson random variable if and only if a point process $\Phi = \{x_{(i)} : i = 1, 2, \dots\} \subset R^d$ is a PPP. In the real plane, the R^d is called d dimensional space. The number of points in discrete sets are independent and have a Poisson distribution:

$$P\{t \text{ points in set } B\} = P\{\Phi(B) = t\} = \frac{\Lambda^t}{t!} \exp(-\Lambda), \quad (1)$$

where the Poisson random variable of density $\lambda(x)$ is the density measure of $\Lambda = \int_B \lambda(x)dx$. It can be said that the PPP is uniform or homogeneous PPP (HPPP), if $\lambda(x)$ is constant ($\lambda(x) = \lambda$) [32]. Especially, the expected number of points in a set B is an density measure which is described below [33]:

$$\Lambda(B) \triangleq E[N(B)], \forall B \in R^d. \quad (2)$$

If $|\cdot|$ is the Lebesgue measure of set B , $N(B)$ has a Poisson distribution with mean $\lambda|B|$ for every compact cluster B . Then, equation (1) turns into:

$$P\{\Phi(B) = t\} = \frac{(\lambda(B))^t}{t!} \exp(-\lambda(B)). \quad (3)$$

The IIoT devices and APs are deployed on the Voronoi tessellation according to the PPP indicated with Φ and density λ and the cluster B is regarded as a two-dimensional Euclidean space [34]. The partition of the plane into n convex polytopes is named as the Voronoi tessellation. The APs in the system are deployed following an independent PPP with density λ_1 . In addition, the IIoT devices are modeled into two categories: D2D transmitting IIoT and D2D receiving IIoT. Also, they are deployed following and independent PPP with densities λ_2 and λ_3 , respectively. This model makes the industrial LiFi network more realistic. Fig. 1 presents an exemplar ultra-dense industrial LiFi network deployment which includes various IIoT devices.

B. LIFI CHANNEL MODEL

Industrial LiFi deployments constitute challenging environments where moving IoT machines may produce high-definition video and other heavy sensor data during

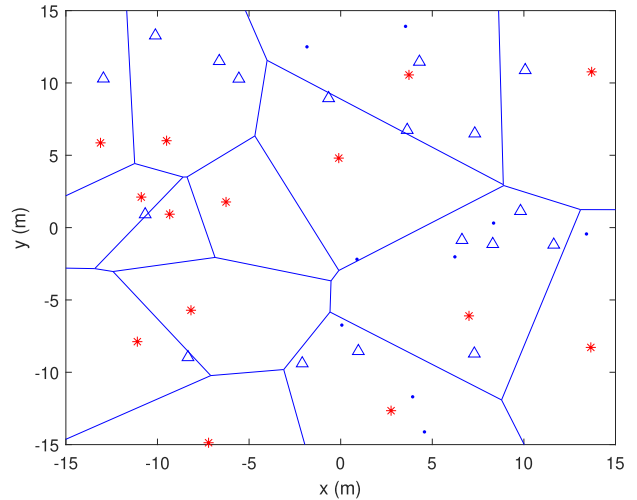


FIGURE 1. PVT ultra-dense LiFi network with the access points (red stars), the D2D transmitting IIoT (blue triangles) and the D2D receiving IIoT (blue dots).

surveying and inspection operations. CoMP-JT for D2D communication in ultra-dense industrial LiFi networks is connected with the Received Optical Intensity (ROI). In other words, the initiation of the connection process is based on measured ROIs. The effect of multiple reflections from the objects and human shadowing are neglected. This means that only line-of-sight (LOS) is taken into account for the LiFi channel model in this study. The insignificant effect of the reflection paths on the ROIs is presented in [30]. According to this assumption, the optical channel gain of the D2D receiving IIoTs from the APs and the D2D transmitting IIoTs can be expressed as [3]:

$$h_i(r_i) = \frac{(m_i + 1)A_r}{2\pi r_i^2} \cos^{m_i}(\varphi_i) T_s g(\psi_i) \cos(\psi_i), \quad (4)$$

where ($i = 1, 2$) represent the direct link and D2D link, respectively, and $ROI_i(r_i) = P_i h_i(r_i)$ can be calculated. In addition, r_i is the distance between the D2D receiving IIoT and a transmitter located point at i , A_r is the receiver effective area, P_i is the transmitted power, ψ_i is the angle of incidence with respect to the axis normal to the receiver surface, φ_i is the angle of irradiance with respect to the axis normal to the transmitter surface, ψ_{con} and $g(\psi_i)$ are the field-of-view (FOV) and concentrator gain, respectively. T_s is the filter transmission and m_i is the Lambertian index described as [3]:

$$m_i = -\frac{\ln(2)}{\ln[\cos(\varphi_{1/2})]}, \quad (5)$$

where $\varphi_{1/2}$ is the semiangle at half illuminance of the transmitter. Further, the gain of the optical concentrator at the receiver is expressed by [3]:

$$g(\psi) = \begin{cases} n^2 / \sin^2(\psi_{con}), & \text{if } 0 < \psi \leq \psi_{con} \\ 0, & \text{if } \psi_{con} \leq \psi, \end{cases} \quad (6)$$

where n is the refractive index.

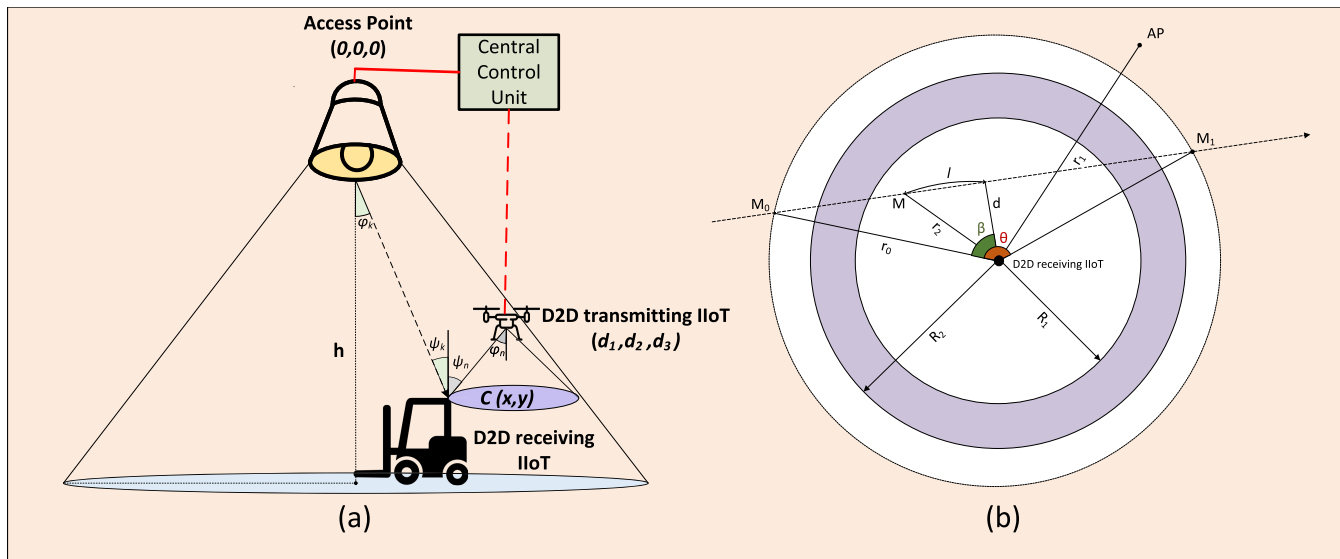


FIGURE 2. (a) Changing of D2D communication range; (b) Relative movement analytical framework.

III. PROBABILITY OF CoMP-JT SCHEME FOR LIFI-BASED D2D COMMUNICATION NETWORKS

Generally, an industrial network consists of multiple cells that are neighbors to each other. The boundaries of these cells delimit their coverage area. That is, ROI in LiFi is the principal criteria for shaping the cell borders [35]. In this work, the transmitter and receiver positions are based on the ‘Scenario 4: Manufacturing Cell’ in LiFi standards, produced by the IEEE 802.11bb Task Group on Light communications [26]. This standard considers multiple robots as IIoT devices in a factory environment. It is assumed that the IIoT devices have their LiFi transmitters/receivers vertically positioned as illustrated in Fig. 2a. It is also assumed that IIoT devices in industrial LiFi networks move in a two-dimensional space. When the CoMP-JT scheme for D2D communication is considered, IIoT devices are initially distributed within the coverage area of the APs as shown in Figure 2a. Thus, an AP represents an umbrella tier and IIoT devices are deployed under this umbrella.

The scenario is composed of a central control unit (CCU) and multiple LiFi transmitters such as in Fig. 2a. The modulated signal is directly sent from the CCU to each transmitter and converted to a LiFi signal. The frames control, signal processing, synchronization, initiating of the scheme and modulation are all carried out at the CCU. Therefore, coordinated transmission can be achieved via the backhaul link. The high-speed connection between CCU and transmitters can be achieved by using optical fiber, Ethernet cable, powerline communication and wireless communication technologies. In order to avoid inter-cell interference, direct-current-biased optical orthogonal frequency division multiplexing (DCO-OFDM) is used in order to realize orthogonal frequency division multiple access (OFDMA) which allows simultaneous transmission by adjacent transmitters.

Using stochastic geometry, it is possible to propose an analytical model for CoMP-JT and evaluate coverage probability of its mobile nodes. Thus, the scenario can be simplified to only one D2D receiving IIoT device together with distributed multiple D2D transmitting IIoT devices. With the D2D receiving IIoT taken as a reference point, then the D2D transmitting IIoT is treated as moving relative to the reference point. Modeling the exact movement of the devices is extremely complicated and will depend on the given scenario and environment. This work will not focus on improving such a movement model. Instead, it is assumed that a mobile node’s motion comprises of straight line segments and the node travels at a constant speed V in each of these segments.

Without loss of generality, the position $\mathbf{x}_t(d_1, d_2, d_3)$ is the location of a D2D transmitting IIoT device and a typical AP is located at the origin. Based on the ROI from each tier, the CoMP-JT or non-coordinated modes can be operated by the D2D receiving IIoT device independently. When the ROI from an AP is sufficiently higher than that from any neighbouring D2D transmitting IIoT device, the D2D receiving IIoT device is only served by the AP. The AP and D2D transmitting IIoT start CoMP-JT to the D2D receiving IIoT when the ROI from the strongest neighbor D2D transmitting IIoT device is comparable to that of the connecting AP. In this circumstance, the CoMP-JT mode is initiated. The CoMP-JT is maintained until the ROI from the D2D transmitting exceeds the ROI from the AP. We focus on whether the D2D transmitting IIoT would keep CoMP-JT with AP rather than the non-coordinated circumstance. The analytical framework of the dynamic CoMP-JT association criterion is designed as follows [36]:

$$1 \leq \frac{\text{ROI}_1(r_1)}{\text{ROI}_2(r_2)} < \eta, \tag{7}$$

where we refer to η as the bias factor (≥ 0 dB) which is the coordination threshold. The bias factor encourages D2D receiving IIoT to connect low-load D2D transmitting IIoT.

Referring to Figure 2b, let's assume that the random trajectory of the strongest D2D transmitting IIoT device is a straight line which is determined by two points M_0 and M_1 . r_0 symbolizes the distance between the M_0 and the typical D2D receiving IIoT device. M_1 is a random point on the dotted circle of radius r_0 centered at the D2D receiving IIoT device. $\theta \in [0, 2\pi]$ is a random orientation which represents the moving direction of the strongest D2D transmitting IIoT device [37]. In this study, we focus on the region where D2D receiving IIoT devices operate in CoMP-JT mode. According to (7), the annular observation region Γ is delimited by the minimum and maximum radii R_1 and R_2 , respectively, that is $\Gamma = \{(r_1, r_2) : r_1 > 0 \text{ and } R_1 < r_2 < R_1\}$. R_1 and R_2 symbolize the minimum and maximum coverage radius of the CoMP-JT scheme in regard to bias factor η ; furthermore, R_1 and R_2 are given in Appendix A.

In terms of assignment policy, the CoMP-JT procedure will trigger when the nearest D2D transmitting IIoT enters into the region Γ . As shown in Figure 2b, d is a distance from the D2D receiving IIoT to the movement trajectory of its nearest D2D transmitting IIoT device. The probability of CoMP-JT can be expressed as the probability that the random trajectory of the D2D transmitting IIoT intersects with the annular. That is, $d \leq R_2$ is the requirement that D2D receiving IIoT initiate in CoMP-JT mode. Let assume that Q shows the probability that D2D receiving IIoT operates in CoMP-JT mode with a neighbor D2D transmitting IIoT.

Firstly, the trajectory of the coordinated D2D transmitting IIoT is a key point of obtaining the distribution of the angle β . As shown in Figure 2b, the angle β in the right triangle is within the interval $[0, \pi/2]$. Based on the definition from [37], angle β can be denoted for various range of θ as follows:

$$\beta = \begin{cases} \theta/2, & \text{if } 0 < \theta < \pi \\ \pi - \theta/2, & \text{if } \pi < \theta < 2\pi, \end{cases} \quad (8)$$

where angle θ is determined by the intersection points between the trajectory of the D2D transmitting IIoT and dotted circle. The distribution of Θ can be expressed as follows:

$$F_{\Theta}(\theta) = \frac{(4\pi - \theta)\theta}{4\pi^2}, \quad 0 < \theta < 2\pi. \quad (9)$$

Together with (8) and (9), the cumulative distribution function (cdf) of B can be derived as:

$$F_B(\beta) = 2\beta/\pi, \quad 0 < \beta < \pi/2. \quad (10)$$

Considering the first-order derivative of (10), the probability density function (pdf) of B is given by [36]:

$$f_B(\beta) = 2/\pi, \quad 0 < \beta < \pi/2. \quad (11)$$

The distance from the D2D receiving IIoT to the initial location of nearest AP and the D2D transmitting IIoT is denoted

as r_1 and r_2 , respectively. In a homogeneous PPP, the pdf of r_1 and r_2 , that is $f_{R_1}(r_1)$ and $f_{R_2}(r_2)$, can be derived as follows:

$$f_{R_1}(r_1) = 2\pi\lambda_1 r_1 e^{-\pi\lambda_1 r_1^2} \quad (12)$$

$$f_{R_2}(r_2) = 2\pi\lambda_2 r_2 e^{-\pi\lambda_2 r_2^2}. \quad (13)$$

By utilization of (4), (7), (12) and (13) we can obtain the probability of CoMP-JT scheme for LiFi-based D2D communication as follows:

$$\begin{aligned} Q &= \mathbb{P}[d \leq R_2] \\ &= \mathbb{P}[r_2 \cos(\beta) \leq \sqrt{\eta Z} r_1 \sin(\psi_2)] \\ &= \mathbb{P}\left[r_2 \leq \frac{\sqrt{\eta Z} r_1 \sin(\psi_2)}{\cos(\beta)}\right] \\ &= \mathbb{E}_{\beta, r_1} \left[1 - \exp\left(-\pi\lambda_2 \frac{\eta Z r_1^2 \sin^2(\psi_2)}{\cos^2(\beta)}\right) \right] \\ &= \mathbb{E}_{\beta} \left[\frac{1}{1 + \left(\frac{\lambda_1}{\lambda_2} \frac{\cos^2(\beta)}{\eta Z \sin^2(\psi_2)}\right)} \right] \\ &= \frac{1}{\sqrt{1 + \frac{\lambda_1}{\lambda_2} \frac{h^2 + (R_2 - R_1)^2}{\eta R_1^2}}}, \end{aligned} \quad (14)$$

where $Z = \frac{P_2 \cos^{m_2+1}(\varphi_2)}{P_1 \cos^{m_1+1}(\varphi_1)}$. It is clear from (14), the probability of the IIoT devices operating in CoMP-JT mode has positive correlation with the ratio of AP and D2D transmitting IIoT density. Larger bias factor η also increases the CoMP-JT probability.

IV. COVERAGE PERFORMANCE OF CoMP-JT SCHEME FOR D2D COMMUNICATION

In the wireless communication systems, the coverage probability is determined by the probability that the signal-to-interference-plus-noise-ratio (SINR) of a randomly located user is more than a predetermined threshold τ [38]. For LiFi-based system, the received SINR expression from i -th tier can be written as:

$$\text{SINR}_i = \frac{R_{pd}^2 h_i^2 P_i^2}{R_{pd}^2 \sum_{j \neq i} h_j^2 P_j^2 + \sigma^2} \quad (15)$$

where R_{pd} is the responsivity of the receiver and σ^2 is the noise variance. The interference can be represented as $I = R_{pd}^2 \sum_{j \neq i} h_j^2 P_j^2$. According to the definition, the coverage probability of the D2D receiving IIoT can be derived as [36]:

$$\begin{aligned} \mathbb{C} &= \mathbb{P}\{\text{SINR} > \tau\} \\ &\stackrel{(a)}{=} \mathbb{P}\{|R_{pd} h_1 P_1 + R_{pd} h_2 P_2|^2 > \tau R_{pd}^2 \sum_{j \neq 1,2} h_j^2 P_j^2 + \tau \sigma^2\} \\ &\stackrel{(b)}{=} \mathbb{E} \left[\exp \left\{ \frac{-\tau \sigma^2}{R_{pd} \sum_{j=1}^2 P_j} \right\} \times \prod_{j=1}^2 \mathcal{L}_I \left(\frac{\tau}{R_{pd} \sum_{j=1}^2 P_j} \right) \right], \end{aligned} \quad (16)$$

where (a) follows the definition of SINR cdf, (b) follows from the definition of the Laplace transform. The Laplace

transform of I is calculated as follows:

$$\begin{aligned} \mathcal{L}_I(s) &= \mathbb{E}[\exp\{-sI\}] \\ &\stackrel{(c)}{=} \mathbb{E}\left[\exp\left\{-sR_{pd}^2 \sum_{j \neq 1,2} h_j^2 P_j^2\right\}\right] \\ &\stackrel{(d)}{=} \exp\left\{-2\pi\lambda_j \int_{r_j}^{\infty} (1 - \mathbb{E}(e^{-sR_{pd}^2 h_j^2 P_j^2})) r dr\right\} \\ &\stackrel{(e)}{=} \exp\left\{-2\pi\lambda_j (sR_{pd} P_j)^2 \int_{(sR_{pd} P_j)^{-1} r_j}^{\infty} \frac{x}{1+x^2} dx\right\}, \end{aligned} \quad (17)$$

where (c) and (d) is derived by using the Laplace Functional of PPP [39], and (e) is derived by replacing $x = (sR_{pd} P_j)^{-1}$. Combining (16) and (17), the coverage probability can be derived as:

$$\begin{aligned} \mathbb{C} &= \mathbb{E}\left[\exp\left\{\frac{-\tau\sigma^2}{R_{pd} \sum_{j=1}^2 P_j}\right\}\right] \\ &\times \prod_{j=1}^2 \exp\left\{-2\pi\lambda_j \left(\frac{\tau R_{pd} P_j}{R_{pd} \sum_{j=1}^2 P_j}\right)^2\right. \\ &\times \left.\int_{(sR_{pd} P_j)^{-1} r_j}^{\infty} \frac{x}{1+x^2} dx\right\}. \end{aligned} \quad (18)$$

To provide a more straightforward expression for the coverage probability for CoMP-JT based D2D communication, we need to obtain the pdfs of D and L (as shown in Figure 2b) and the joint pdf of $R_c = (R_0, R_1)$. From the geometric configuration in Figure 2b, we get:

$$r_2 = \sqrt{d^2 + l^2}, \quad R_1 < r_2 < R_2. \quad (19)$$

Based on (11) and (13), the pdf of D can be derived as:

$$f_D(d) = \frac{2}{\pi\sqrt{r_0^2 - d^2}}, \quad 0 < d < R_2. \quad (20)$$

According to the definition of the D2D transmitting IIoT's trajectory, the pdf of L is obtained for different range of variable d :

$$f_L(l) = \begin{cases} (\sqrt{R_2^2 - d^2} - \sqrt{R_1^2 - d^2})^{-1}, & \text{if } 0 < d < R_1 \\ (\sqrt{R_2^2 - d^2})^{-1}, & \text{if } R_1 < d < R_2. \end{cases} \quad (21)$$

According to PPP properties, the probability of the distance between the D2D receiving IIoT and its nearby transmitters can be derived. Especially, the joint pdf of R_c can be derived as:

$$f_{R_c}(r_0, r_1) = 4\pi^2 \lambda_1 \lambda_2 r_0 r_1 \exp\{-\pi(\lambda_1 r_1^2 + \lambda_2 r_0^2)\}. \quad (22)$$

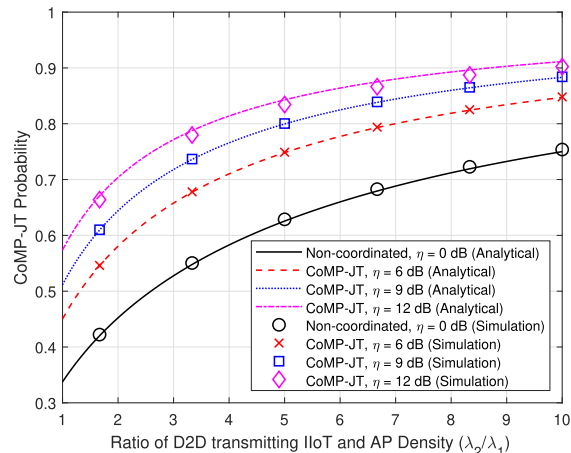


FIGURE 3. CoMP-JT probability of D2D receiving IIoT vs. ratio of D2D transmitting IIoT and AP density.

By combining (19), (20), (21) and (22), then substituting in (18), we compute the approximate coverage probability of a randomly located CoMP-JT based D2D device in industrial LiFi network as in (23), shown at the bottom of the page.

V. NUMERICAL RESULTS AND DISCUSSIONS

In this section, we discuss the performance metrics of the CoMP-JT scheme for D2D communication in industrial LiFi networks and compare with the Monte Carlo method-based simulation results. Unless otherwise stated, the simulation environment is considered with dimensions: $30 \times 30 \times 5 \text{ m}^3$ and the semiangle at half illuminance of the transmitters are selected as equal to 60° . Moreover, the relationship between transmit powers is set as $P_1 = 25P_2 = 25 \text{ W}$, the tier densities $\lambda_1 = 0.5\lambda_2 = 1 \text{ [node/m}^2\text{]}$, and the bias factor $\eta = 6 \text{ dB}$ for this illustration environment. The height of the D2D receiving IIoTs and the D2D transmitting IIoTs from the ground has been taken as 2 m and 3 m, respectively.

Figure 3 shows the relationship between CoMP-JT probability and different densities of APs and D2D transmitting IIoTs (λ_2/λ_1). The figure shows that the denser D2D transmitting IIoT device deployment increase the CoMP-JT probability. This is because the IIoT deployment gets denser as λ_2 increases, which means that transition between the AP and the D2D transmitting IIoT is initiated more. On the other hand, the probability growth will eventually slow down and stabilize when the density of D2D transmitting IIoT is much higher than that of APs in ultra-dense industrial LiFi network. Additionally, the CoMP-JT probability increases with the bias factor. As a result, increasing the D2D transmitting IIoT

$$\begin{aligned} \mathbb{C} &= \int_{\Gamma} \left[\exp\left\{\frac{-\tau\sigma^2}{R_{pd} \sum_{i=1}^2 P_i}\right\} \times \prod_{j=1}^2 \exp\left\{-2\pi\lambda_j \left(\frac{\tau P_j}{\sum_{i=1}^2 P_i}\right)^2 \times \int_{\left(\frac{\tau P_j}{\sum_{i=1}^2 P_i}\right)^{-1} r_j}^{\infty} \frac{r}{1+r^2} dr\right\}\right. \\ &\times \left. f_L(l) f_D(d) f_{R_c}(r_0, r_1) dl dd r_0 dr_1 \right] \end{aligned} \quad (23)$$

density is inefficient after certain thresholds. The analytical results of the CoMP-JT probability which are obtained in Section III fit well with the Monte Carlo method-based simulation results.

It should be noted that the 2-D space models the statistical position of the access points but not their height above the reference plain. This is representative as access points have a fixed heights but their location is randomly distributed. To consider a complete 3-D space, the effect of the transmitting IIoT heights on the CoMP-JT probability is presented next. As can be seen from (14), the height of the D2D transmitting IIoT devices, d_3 , has an indirect impact on the system performance via the minimum and maximum coverage radius of the CoMP-JT scheme, R_1 and R_2 . In Fig. 4, three different densities of APs and D2D transmitting IIoTs, λ_2/λ_1 , and different D2D transmitting IIoT heights, d_3 , are compared in terms of the CoMP-JT probability. The different D2D transmitting IIoT heights do not lead to a dramatic change in the CoMP-JT probabilities. As the height of transmitters from the ground increases, it is expected that the coverage area of the transmitters increases as well. Thus, an increase in height is a reason for the increase in CoMP-JT probability shown in Fig.4. On the other hand, the ROI of the D2D receiving IIoT decreases as the transmitter height is increased due to an increase in the Euclidean distance between them. Therefore, the change in CoMP-JT probability will be limited because of the trade-off between coverage area and ROI.

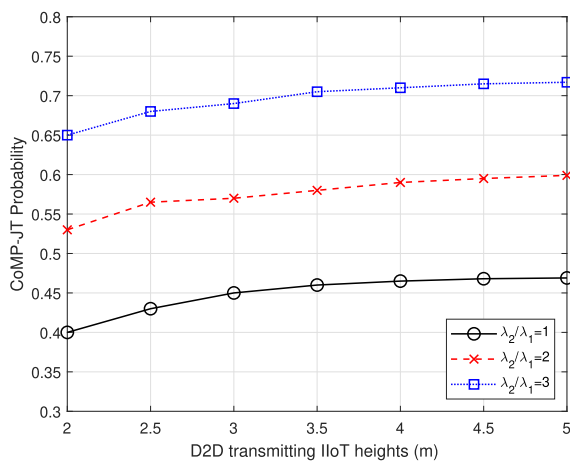


FIGURE 4. CoMP-JT probability for different D2D transmitting IIoT heights in terms of different transmitting density ratios.

In this study, it is preferred that the transmitting IIoT vertical heights follow fixed values rather than PPP. Introducing randomness to the height of a LiFi AP makes the distance distribution between a typical user and a LiFi AP extremely cumbersome and difficult to model. Varying access point height is not only unrealistic but does not have any significant impact on the CoMP-JT probability as Fig 4 shows. Also, this framework is in line with previous research results, especially in terms of fixed vertical height values [22].

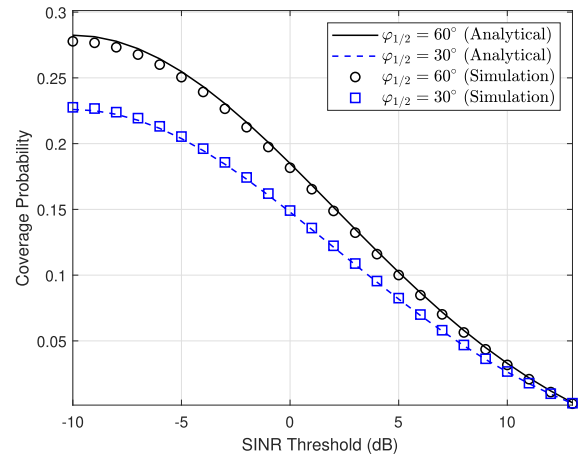


FIGURE 5. Coverage probability in terms of semiangle at half illuminance of the transmitters.

Figure 5 shows the results for different semiangle at half illuminance of the transmitters which relates directly to the coverage area. Decreasing the SINR threshold and semiangle at half illuminance adversely affect the coverage area. This is simply because a larger semiangle at half illuminance provides a wider coverage area, the source optical power is spread over a much wider space. The results show that the analytical approximation in (23) matches the Monte Carlo simulations well. However, there are tiny gaps on different sides of the different semiangle at half illuminance values. This is due to the nature of the simulation technique and approximation error in the analytical expression.

The Monte Carlo method-based simulation results match quite well with the obtaining analytical expression results, namely, they verify each other. The validation of the analytical results by the simulation results is provided better insights for the system design of the CoMP-JT scheme for D2D communication in ultra-dense industrial LiFi networks. For example, the density of the IIoT can be estimated by using the analytical expression of the CoMP-JT probability when the value of the bias factor in a designed space is known.

For better comparison, two alternatives schemes are introduced, namely, non-coordinated maximum-received-optical-intensity-based (NC-MROI) and non-coordinated D2D-transmitting-IIoT-bias-based (NC-DB). In NC-MROI, the D2D receiving IIoTs connect to strongest D2D transmitting IIoT or AP without any bias factor ($\eta = 0$). That is, the D2D receiving IIoT is served by the most powerful transmitter in terms of ROI. In the other scheme, the D2D receiving IIoTs prefer association to the D2D transmitter IIoTs in NC-DB scheme. The positive bias to tier 2 association is defined as $\eta = 6$ dB. As shown in Figure 6, the coverage probability of the CoMP-JT scheme has better coverage performance than others with different SINR threshold. The CoMP-JT scheme can improve the coverage performance of the IIoTs by about 5% when $\tau = 0$ dB.

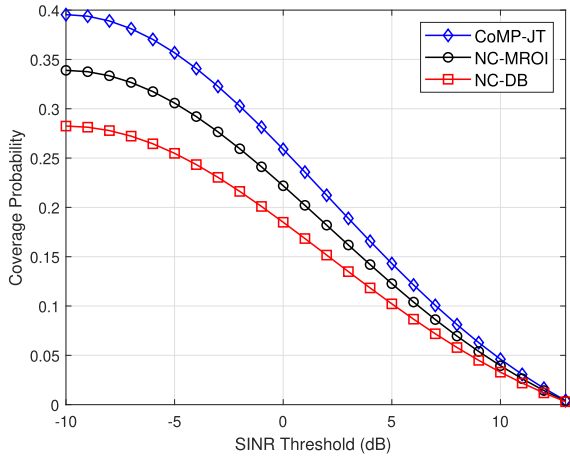


FIGURE 6. Comparison of the coverage probability of alternative schemes.

VI. CONCLUSION

In this work, the key performance metrics for the CoMP-JT scheme for D2D communication in ultra-dense industrial LiFi networks are analyzed. Based on semiangle at half illuminance, the analytical model for the coverage areas of the D2D communication is presented. In addition, the CoMP-JT probability and coverage probability are obtained as analytical expressions which are functions of the system parameters. From the analytical expressions, it is clear that AP density, IIoT density, and bias factor are crucial parts of the CoMP-JT scheme for D2D communication. In addition, simulation results match well with the theoretical models presented. The obtaining results are valuable in practical industrial LiFi design and development.

APPENDIX A

Without loss of generality, the position $\mathbf{x}_t(d_1, d_2, d_3)$ is the location of a D2D transmitting IIoT device and a typical AP is located at the origin. In regard to the ROI, the radius of the D2D transmitting IIoT can be determined as,

$$C = \{(x, y) \in \mathbb{R}^2 \mid \text{ROI}_1(r_1) = \eta \text{ROI}_2(r_2)\}. \quad (24)$$

Thus, the coverage boundary of the D2D communication range forms a cluster of bias-based ROI points in (24). These points help to calculate the parameters in an industrial LiFi network. For a D2D receiving IIoT located at $(x, y) \in \mathbb{R}^2$ and the height from the ground is h , the distance from the D2D receiving IIoT to the AP, and the D2D transmitting IIoT are given, respectively, by [40], [41],

$$r_1 = \sqrt{x^2 + y^2 + h^2}, \quad (25)$$

$$r_2 = \sqrt{(x - d_1)^2 + (y - d_2)^2 + (h - d_3)^2}. \quad (26)$$

In addition, $\cos(\varphi_1) = \cos(\psi_1) = \frac{h}{\sqrt{x^2 + y^2 + h^2}}$ and $\cos(\varphi_2) = \cos(\psi_2) = \frac{h - d_3}{\sqrt{(x - d_1)^2 + (y - d_2)^2 + (h - d_3)^2}}$ are considered because IIoT device faces are directed upward.

By substituting (25) and (26) into (24), we obtain,

$$W_i \cdot (x^2 + y^2 + h^2)^{\widehat{m}} - [(x - d_1)^2 + (y - d_2)^2 + (h - d_3)^2] = 0 \quad (27)$$

where, $W_i = \left(\frac{\eta P_2(m_2+1)(h-d_3)^{m_2+1}}{P_1(m_1+1)h^{m_1+1}} \right)^{\frac{2}{m_2+3}}$, $\widehat{m} = \frac{m_1+3}{m_2+3}$. At this

point, it is assumed that the Lambertian index of the transmitters in the system are identical. Thus, both the AP and the D2D transmitting IIoT share an equal Lambertian index ($m_1 = m_2$), \widehat{m} equals 1. Thus, the equation of a circle can be stated as the defined function in (27) very well. The radius, R_i is calculated as:

$$R_i = \sqrt{\frac{W_i(d_1^2 + d_2^2)}{(1 - W_i)^2} + \frac{W_i h^2 - (h - d_3)^2}{(1 - W_i)}}. \quad (28)$$

In order to obtain certain calculable results and because of stochastic geometry specifications, the distance between AP and D2D transmitting IIoT in the 2D scenario can be approximated as $\mathbb{E}[|L(\mathbf{X}_1, \mathbf{X}_2)|] \cong \sqrt{d_1^2 + d_2^2} = \frac{1}{2\sqrt{\lambda_1}}$ [40].

ACKNOWLEDGMENT

For the purpose of open access, the authors have applied a Creative Commons Attribution (CC BY) licence to any Author Accepted Manuscript version arising from this submission.

REFERENCES

- [1] Cisco Service Provider Wi-Fi: A Platform for Bus, Innovation and Revenue Generation, CISCO, San Jose, CA, USA, Nov. 2012.
- [2] F. Jeldling, "Ericsson mobility report," Ericsson, Stockholm, Sweden, Tech. Rep., Nov. 2020.
- [3] Z. Ghassemlooy, W. Popoola, and S. Rajbhandari, *Optical Wireless Communications: System and Channel Modelling With MATLAB*. Boca Raton, FL, USA: CRC Press, 2019.
- [4] *LTE Device to Device Proximity Services; User Equipment (UE) Radio Transmission and Reception*, document 3GPP 36.877, 3GPP, 2014.
- [5] *Requirements for Evolved UTRA (E-UTRA) and Evolved UTRAN (E-UTRAN)*, Version 8.0.0, Release 8, 3GPP, 2009.
- [6] H. Zhang, W. Ding, J. Song, and Z. Han, "A hierarchical game approach for visible light communication and D2D heterogeneous network," in *Proc. IEEE Global Commun. Conf. (GLOBECOM)*, Dec. 2016, pp. 1–6.
- [7] P. Mach, Z. Becvar, M. Najla, and S. Zvanovec, "Combination of visible light and radio frequency bands for device-to-device communication," in *Proc. IEEE 28th Annu. Int. Symp. Pers., Indoor, Mobile Radio Commun. (PIMRC)*, Oct. 2017, pp. 1–7.
- [8] Z. Becvar, M. Najla, and P. Mach, "Selection between radio frequency and visible light communication bands for D2D," in *Proc. IEEE 87th Veh. Technol. Conf. (VTC Spring)*, Jun. 2018, pp. 1–7.
- [9] N. Raveendran, H. Zhang, D. Niyato, F. Yang, J. Song, and Z. Han, "VLC and D2D heterogeneous network optimization: A reinforcement learning approach based on equilibrium problems with equilibrium constraints," *IEEE Trans. Wireless Commun.*, vol. 18, no. 2, pp. 1115–1127, Feb. 2019.
- [10] H. Zhang, W. Ding, F. Yang, J. Song, and Z. Han, "Resource allocation in heterogeneous network with visible light communication and D2D: A hierarchical game approach," *IEEE Trans. Commun.*, vol. 67, no. 11, pp. 7616–7628, Nov. 2019.
- [11] M. Najla, P. Mach, Z. Becvar, P. Chvojka, and S. Zvanovec, "Efficient exploitation of radio frequency and visible light communication bands for D2D in mobile networks," *IEEE Access*, vol. 7, pp. 168922–168933, 2019.
- [12] M. Najla, P. Mach, and Z. Becvar, "Deep learning for selection between RF and VLC bands in device-to-device communication," *IEEE Wireless Commun. Lett.*, vol. 9, no. 10, pp. 1763–1767, Oct. 2020.

- [13] Z. Becvar, R.-G. Cheng, M. Charvat, and P. Mach, "Mobility management for D2D communication combining radio frequency and visible light communications bands," *Wireless Netw.*, vol. 26, no. 7, pp. 5473–5484, Oct. 2020.
- [14] S. V. Tiwari, A. Sewaiwar, and Y.-H. Chung, "Optical repeater assisted visible light device-to-device communications," *Int. J. Electron. Commun. Eng.*, vol. 10, no. 2, pp. 206–209, 2016.
- [15] Y. Liu, Z. Huang, W. Li, and Y. Ji, "Game theory-based mode cooperative selection mechanism for device-to-device visible light communication," *Opt. Eng.*, vol. 55, no. 3, Mar. 2016, Art. no. 030501.
- [16] Z. N. Chaleshtori, S. Zvanovec, Z. Ghassemlooy, O. Haddad, and M.-A. Khalighi, "Impact of receiver orientation on OLED-based visible-light D2D communications," in *Proc. 17th Int. Symp. Wireless Commun. Syst. (ISWCS)*, Sep. 2021, pp. 1–6.
- [17] Z. N. Chaleshtori, S. Zvanovec, Z. Ghassemlooy, and M.-A. Khalighi, "Visible light communication with OLEDs for D2D communications considering user movement and receiver orientations," *Appl. Opt.*, vol. 61, no. 3, pp. 676–682, 2022.
- [18] P. Kumar and K. P. Sharma, "Challenges and applications of Li-Fi in D2D communication," in *Proc. Int. Conf. Commun., Control Inf. Sci. (ICCISc)*, Jun. 2021, pp. 1–6.
- [19] M. Xu, X. Tao, F. Yang, and H. Wu, "Enhancing secured coverage with CoMP transmission in heterogeneous cellular networks," *IEEE Commun. Lett.*, vol. 20, no. 11, pp. 2272–2275, Nov. 2016.
- [20] C. Chen, D. Tsonev, and H. Haas, "Joint transmission in indoor visible light communication downlink cellular networks," in *Proc. IEEE Globecom Workshops (GC Wkshps)*, Dec. 2013, pp. 1127–1132.
- [21] M. S. Demir, F. Miramirkhani, and M. Uysal, "Handover in VLC networks with coordinated multipoint transmission," in *Proc. IEEE Int. Black Sea Conf. Commun. Netw. (BlackSeaCom)*, Jun. 2017, pp. 1–5.
- [22] L. Yin and H. Haas, "A tractable approach to joint transmission in multi-tier visible light communication networks," *IEEE Trans. Mobile Comput.*, vol. 18, no. 10, pp. 2231–2242, Oct. 2019.
- [23] L. Yin, X. Wu, and H. Haas, "SDMA grouping in coordinated multi-point VLC systems," in *Proc. IEEE Summer Top. Meeting Ser. (SUM)*, Jul. 2015, pp. 169–170.
- [24] B. G. Guzman, A. A. Dowhuszko, V. P. G. Jimenez, and A. I. Perez-Neira, "Cooperative transmission scheme to address random orientation and blockage events in VLC systems," in *Proc. 16th Int. Symp. Wireless Commun. Syst. (ISWCS)*, Aug. 2019, pp. 351–355.
- [25] C. Chen and H. Haas, "Performance evaluation of downlink cooperative multipoint joint transmission in LiFi systems," in *Proc. IEEE Globecom Workshops (GC Wkshps)*, Dec. 2017, pp. 1–6.
- [26] M. Uysal, F. Miramirkhani, T. Baykas, and K. Qaraqe, "IEEE 802.11bb reference channel models for indoor environments," *Tech. Rep.*, 2018.
- [27] H. Haas, L. Yin, Y. Wang, and C. Chen, "What is LiFi?" *J. Lightw. Technol.*, vol. 34, no. 6, pp. 1533–1544, Mar. 15, 2016.
- [28] H. Haas, L. Yin, C. Chen, S. Videv, D. Parol, E. Poves, H. Alshaer, and M. S. Islam, "Introduction to indoor networking concepts and challenges in LiFi," *J. Opt. Commun. Netw.*, vol. 12, no. 2, pp. A190–A203, Feb. 2020.
- [29] C. Chen, D. Basnayaka, and H. Haas, "Downlink SINR statistics in OFDM-based optical attocell networks with a Poisson point process network model," in *Proc. IEEE Global Commun. Conf. (GLOBECOM)*, Dec. 2015, pp. 1–6.
- [30] C. Chen, D. A. Basnayaka, and H. Haas, "Downlink performance of optical attocell networks," *J. Lightw. Technol.*, vol. 34, no. 1, pp. 137–156, Jan. 1, 2016.
- [31] G. Last and M. Penrose, *Lectures on the Poisson Process*, vol. 7, Cambridge, U.K.: Cambridge Univ. Press, 2017.
- [32] S. Wu *et al.*, "Stochastic geometry-based analysis of emerging network technologies: From millimeter-wave cellular to nano-optical networks," Ph.D. thesis, Dept. Elect. Eng., State Univ. New York Buffalo, Buffalo, NY, USA, 2018.
- [33] M. Haenggi, *Stochastic Geometry for Wireless Networks*. Cambridge, U.K.: Cambridge Univ. Press, 2012.
- [34] A. R. Khamesi and M. Zorzi, "Energy and area spectral efficiency of cell zooming in random cellular networks," in *Proc. IEEE Global Commun. Conf. (GLOBECOM)*, Dec. 2016, pp. 1–6.
- [35] M. D. Soltani, A. A. Purwita, Z. Zeng, H. Haas, and M. Safari, "Modeling the random orientation of mobile devices: Measurement, analysis and LiFi use case," *IEEE Trans. Commun.*, vol. 67, no. 3, pp. 2157–2172, Mar. 2019.
- [36] X. Tang, X. Xu, T. Svensson, and X. Tao, "Coverage performance of joint transmission for moving relay enabled cellular networks in dense urban scenarios," *IEEE Access*, vol. 5, pp. 13001–13009, 2017.
- [37] X. Yan, N. Mani, and Y. A. Sekercioglu, "A traveling distance prediction based method to minimize unnecessary handovers from cellular networks to WLANs," *IEEE Commun. Lett.*, vol. 12, no. 1, pp. 14–16, Jan. 2008.
- [38] A. B. Ozyurt, M. Basaran, and L. Durak-Ata, "Impact of self-configuration on handover performance in green cellular networks," in *Proc. Adv. Wireless Opt. Commun. (RTUWO)*, pp. 194–197, 2018.
- [39] F. Baccelli and B. Baszczyszyn, *Stochastic Geometry and Wireless Networks*, vol. 1. Norwell, MA, USA: Now Publishers, 2009.
- [40] A. B. Ozyurt and W. O. Popoola, "Mobility management in multi-tier LiFi networks," *J. Opt. Commun. Netw.*, vol. 13, no. 9, pp. 204–213, Sep. 2021.
- [41] A. B. Ozyurt, I. Tinnirello, and W. O. Popoola, "Modelling of multi-tier handover in LiFi networks," in *Proc. IEEE Global Commun. Conf. (GLOBECOM)*, Dec. 2021, pp. 1–6.



AHMET BURAK OZYURT (Graduate Student Member, IEEE) received the double B.Sc. degrees in electronics-communication engineering and management engineering from Istanbul Technical University, Turkey, in 2018, and the M.Sc. degree in information and communication engineering from the Informatics Institute, Istanbul Technical University, in 2020. He is currently pursuing the Ph.D. degree with The University of Edinburgh, U.K.

He was with Ericsson, Turkey, working as a Networks Researcher. Since August 2020, he has been with The University of Edinburgh, where he is a Marie Curie Early-Stage Researcher. His paper "Mobility Management in Multi-Tier LiFi Networks," has published in IEEE/OSA JOURNAL OF OPTICAL COMMUNICATIONS AND NETWORKING was appreciated with the Peter Grant Award for the best student-led paper which is given by The University of Edinburgh. His research interests include energy efficiency in cellular networks and optical wireless communication.



WASIU O. POPOOLA (Senior Member, IEEE) received the degree (Hons.) in electronic and electrical engineering from Obafemi Awolowo University, Ile-Ife, Nigeria, in 2003, and the M.Sc. and Ph.D. degrees in optical communication engineering from Northumbria University, Newcastle upon Tyne, U.K., in 2006 and 2009, respectively.

He is currently a University Senior Lecturer and the Deputy Director of learning and teaching with the School of Engineering, The University of Edinburgh, Edinburgh, U.K. He has authored or coauthored more than 110 journal articles/conference papers/patent and over seven of those are invited articles. He has also coauthored the book *Optical Wireless Communications: System and Channel Modeling with MATLAB* and many other book chapters. One of his journal articles ranked No. 2 in terms of the number of full text downloads within IEEE Xplore, in 2008, from the hundreds of articles has been publishing by *IET Optoelectronics*, since 1980. He has coauthored another article with one of his Ph.D. students has received the Best Poster Award at the 2016 IEEE ICSAE Conference. He is a Science Communicator appearing in science festivals and on "BBC Radio 5live Science" Program, in October 2017. His publications have more 6200 citations and a H-index of 34 on Google Scholar. His research interests include digital and optical communications, including VLC, FSO, and fiber communications.

Dr. Popoola is a fellow of the Institute of Engineering Technology (FIET) and a fellow of the Higher Education Academy (FHEA). He was an Invited Speaker at various events, including the 2016 IEEE Photonics Society Summer Topicals. He is an Associate Editor of IEEE Access journal.

...